Journal of Integrative Neuroscience

J. Integr. Neurosci. **2025**; 24(6): 38100
https://doi.org/10.31083/JIN38100

Original Research

Harmine-mediated Reduction of Bone Cancer Pain in Rats Correlates With Suppressed DYRK1A/NF-κB Signaling Axis

Shuyao Zhang[1,†], Shang Zheng[2,†], Jia Jin[1], Yuhua Li[2], Liping Chen[2], Junjie Lin[2], Ming Yao[2,*], Longsheng Xu[2,*]

[1]College of Life Sciences and Medicine, Zhejiang Sci-Tech University, 310018 Hangzhou, Zhejiang, China
[2]Department of Anesthesiology and Pain Research Center, Jiaxing University Affiliated Hospital, The First Hospital of Jiaxing, 314001 Jiaxing, Zhejiang, China
*Correspondence: jxyaoming@zjxu.edu.cn (Ming Yao); xlsh2468@zjxu.edu.cn (Longsheng Xu)
†These authors contributed equally.
Academic Editor: Parisa Gazerani
Submitted: 16 February 2025 Revised: 5 April 2025 Accepted: 27 April 2025 Published: 23 June 2025

Abstract

Background: Bone cancer pain (BCP) is a prevalent chronic pain condition and a common clinical symptom in patients with advanced cancer. It significantly affects the mobility and quality of life of patients; however, current treatments offer limited efficacy. Harmine, a beta-carboline alkaloid extracted from *Peganum harmala*, exhibits anti-inflammatory, anxiolytic, analgesic, and neuroprotective properties. However, its antinociceptive properties and mechanisms in BCP models remain unclear. This study aimed to systematically investigate the analgesic effects of Harmine in rats with BCP and explore its underlying molecular mechanisms. **Methods**: Using databases such as SwissTargetPrediction and Polypharmacology Browser, molecular docking analysis, behavioral tests, and biochemical analysis, we comprehensively evaluated the effects of Harmine in the BCP model. **Results**: The results demonstrated that Harmine significantly alleviated BCP induced by Luciferin-Malignant Atypical Discrete Breast 106 cells (LUC-MADB106) in a dose-dependent manner. Intrathecal administration of Harmine significantly inhibited the upregulation of dual-specificity tyrosine phosphorylation-regulated kinase 1A (DYRK1A) expression and the activation of the nuclear factor kappa-light-chain-enhancer of activated B cells (NF-κB) pathway in the spinal cord dorsal horn (SCDH) of rats with bone cancer. **Conclusions**: These findings suggest that Harmine has significant therapeutic potential for alleviating BCP hyperalgesia, providing a foundation for the future development of new drugs targeting BCP.

Keywords: bone cancer pain; Harmine; DYRK1A/NF-κB signaling pathway; spinal cord dorsal horn

1. Introduction

Bone cancer pain (BCP) is chronic bone pain caused by malignant tumors in bone metastatic sites and is one of the most common clinical symptoms in patients with advanced cancer. Approximately 75% of patients with metastatic cancer experiencing moderate-to-severe BCP [1]. Despite the availability of various clinical methods [2–4], such as surgical treatment, radiotherapy, and interventional therapies, approximately 50% of pain symptoms in patients with metastatic cancer remain inadequately controlled, leading to significant physical and mental suffering and a severe decline in quality of life [5]. The effective control of cancer pain remains a major challenge in pain research [6]. Current treatments for BCP and other cancer-related pain primarily include nonsteroidal anti-inflammatory drugs, opioids, and bisphosphonates. However, these drugs are often ineffective for moderate-to-severe cancer pain, fail to provide adequate pain relief, and are associated with issues such as safety concerns, addiction, drug tolerance, and severe adverse reactions and side effects [7–10]. Therefore, there is a critical need to find safe and effective new drugs for BCP with minimal side effects and to conduct in-depth research into their mechanisms, which holds significant theoretical and clinical value.

Recent studies have identified several signaling pathways that mediate these pathological processes, including the nuclear factor kappa-light-chain-enhancer of activated B cells (NF-κB) pathway, which plays a pivotal role in inflammation and pain sensitization [11,12]. NF-κB is a crucial transcription factor that plays a key role in regulating immune responses, producing inflammatory cytokines, and activating glial cells. Dysregulation of this pathway has been linked to a range of chronic pain conditions, including BCP [13,14], where its activation in the spinal cord dorsal horn (SCDH) promotes pain sensitization and neuroinflammation [15]. Furthermore, dual-specificity tyrosine phosphorylation-regulated kinase 1A (DYRK1A), a protein kinase that regulates inflammation and neuronal plasticity, has been identified as a potential upstream regulator of NF-κB signaling. Elevated DYRK1A expression has been observed in various chronic pain models, and DYRK1A inhibition has been proposed as a promising strategy to attenuate neuroinflammation and alleviate pain [16].

Harmine is a beta-carboline alkaloid extracted from *Peganum harmala L.* and is known for its pharmacological activities, including anti-inflammatory, antidiabetic, antitumor, and antibacterial properties [17]. Harmine has been used in the treatment of neurodegenerative diseases,

such as Parkinson's and Alzheimer's, primarily because of its ability to reduce inflammatory mediators and oxidative stress while enhancing the activity of mitochondrial respiratory complexes, thereby providing neuroprotection [18]. In South America, Ayahuasca is commonly used to treat depression and anxiety, of which Harmine is one of the main components [19]. A recent research has demonstrated that Harmine can alleviate anxiety by inhibiting neuroinflammation and restoring neuronal plasticity in the basolateral amygdala [20]. A recent study has shown that Harmine can mitigate neurotoxicity in neurodegenerative diseases by inhibiting DYRK1A [21]. Moreover, Harmine effectively suppresses neuroinflammation by modulating the TLR4/NF-κB p65 signaling pathway, an effect also mediated through its inhibition of DYRK1A [22]. Furthermore, Harmine is capable of disrupting neurite formation and regulating the dynamics of Th17 and regulatory T cells, effects that are mediated through its inhibition of DYRK1A [23,24]. Moreover, a study has found that Ayahuasca has significant analgesic effects on both acute and chronic pain. Analysis of the content of Harmine in Ayahuasca revealed that direct administration of Harmine provided more effective analgesic effects [25]. However, the role of Harmine in relieving BCP has not been explored, and its potential mechanisms for providing analgesic effects in BCP require further investigation.

This study aimed to investigate the therapeutic potential of Harmine in BCP treatment and demonstrate its underlying molecular mechanisms. Using a rat model of BCP, we evaluated the analgesic effects of Harmine using behavioral tests, bioluminescence imaging, and biochemical analyses. Our study provides new insights into the role of Harmine as a potential therapeutic agent for BCP and contributes to the identification of novel targets for the treatment of cancer-related pain.

2. Methods

2.1 Drugs and Administration

Harmine (purity $\geq$99.0%) was obtained from MedChemExpress (MCE, HY-N0737, Shanghai, China) and dissolved in distilled water containing 5% Dimethyl Sulfoxide (DMSO, ST038, Beyotime Biotechnology, Shanghai, China), with ultrasound used to facilitate dissolution. DYRK1-IN-1 (purity $\geq$99.1%) was obtained from MCE (HY-132308) and dissolved in distilled water containing 5% DMSO, using sonication to aid dissolution. Pyrrolidinedithiocarbamate ammonium (PDTC, purity $\geq$98.0%) was obtained from MCE (HY-18738) and dissolved in distilled water. Pentobarbital sodium was obtained from Merck (50 mg/kg, 11715, Darmstadt, Germany), dissolved in saline, and administered via intraperitoneal injection. DYRK1-IN-1, PDTC (120 µg/10 µL) [26], and varying concentrations of Harmine (MCE, HY-N0737A, 25, 100, and 400 µg/kg, administered once daily at a volume of 10 µL per dose) were injected intrathecally for 6 consecutive days. Each drug was freshly prepared prior to the experiment.

2.2 Animals

Female Sprague-Dawley rats, weighing 160–180 g, were obtained from the Vital River Laboratory Animal Technology Company, Beijing, China. The rats were housed under controlled conditions, with four rats per cage. The rats were kept under a 12-h light/dark cycle (12:12 h) with free access to water and standard laboratory chow diet. Prior to the commencement of the study, the rats were acclimatized for a 2–5-day period to adjust to the experimental environment. All animal experiments were conducted between 8:00 AM and 8:00 PM to minimize stress in the experimental animals. These experiments were approved by the Institutional Animal Care and Use Committee of Jiaxing University (Ethical Approval No. JUMC2021-093) and were conducted in strict adherence to the guidelines set forth by the International Association for the Study of Pain for the care and use of laboratory animals.

2.3 Establishment of the BCP Model

Lentivirus-infected Malignant Atypical Discrete Breast (MADB) 106 cells, which originated from the MADB 106 breast cancer cell line (Procell, Wuhan, China), were used to establish stable cell lines. These stable luciferase-expressing MADB 106 cells (LUC-MADB 106) were used for BCP modeling. All cell lines were validated to confirm their identities using species-specific PCR methods. Mycoplasma contamination was ruled out using a detection kit from EallBio (03.17012DB, Beijing, China), and negative results ensured the purity and quality of the cell lines used.

The BCP model was established as described in previous studies [27,28]. All rats involved in the experiment were randomly assigned to the sham operation group or model group. Initially, the rats were anesthetized via intraperitoneal injection of 1% pentobarbital sodium solution (50 mg/kg). Once anesthetized, the rats were positioned in the supine position, and a small hole was drilled into the tibial plateau of the left hind limb of each rat. Using 25µl microsyringe (RonMark, Shanghai, China), either LUC-MADB 106 cells (10 µL, 1×10^6 cells/mL) or inactivated cells (10 µL, 1×10^6 cells/mL) were injected into the medullary cavity. The needle remained in place for 1 min before withdrawal, after which the needle hole was sealed with bone wax and sterilized using an iodophor. After the surgical procedure, the rats were placed on a heating pad to maintain their body temperature until they regained consciousness.

2.4 Behavioral Assessment

Von Frey filaments (BME-404, produced by the Institute of Biological Sciences at the Chinese Academy of Med-

ical Sciences, Yunnan, China) were used to assess mechanical pain sensitivity in the experimental rats. These evaluations were performed on the day before the BCP model establishment and on days 3, 6, 9, 12, 15, and 18 after modeling. Prior to testing, the rats were acclimatized in a 20 × 10 × 10 cm plexiglass chamber that minimized their limb movement. The acclimatization period lasted for 3 days, with each session lasting for 20–30 min. Using Dixon's up-and-down method, the following weights were selected for stimulation: 1.4, 2.0, 4.0, 6.0, 8.0, 10.0, 15.0, and 26.0 g fiber filaments. The left hind paw was stimulated with a 6.0 g filament. A positive response, indicated by paw withdrawal or foot licking, was marked as "X", while no response was recorded as "O". After a positive response, a filament with a lower strength was used for the next stimulation. If no response was observed, a filament with a higher strength was used for subsequent stimulation. A 50% foot-withdrawal threshold formula was used to determine the pain threshold. In cases where the sequences "OX" or "XO" occurred, four consecutive measurements were recorded, and the last strength level was noted.

Gait Analysis: We utilized the CatWalk gait analysis system, model ZS-BT/S, sourced from Beijing Zhongshi Science & Technology (Beijing, China), to assess the pain behavioral effects in two groups of rats: the sham surgery group and the model group. The rats were trained to walk through a closed channel, with the bottom section consisting of a glass plate. A fluorescent tube was positioned beneath the plate, casting green light onto the glass surface to allow for detailed tracking of the rats' footprints and movement patterns. As the rats walked across the glass plate, their paws contacted the surface, reflecting green light, which enabled the capture of footprint images and the measurement of footprint intensity. Prior training was necessary to ensure that the rats could navigate the passage at a consistent and uninterrupted speed during the formal data collection phase. The following two key indicators were used to assess the impact of pain on rat behavior: (1) footprint area and (2) average footprint intensity. The data are expressed as the ratio of the left hindlimb to the right hindlimb, which helped mitigate the influence of confounding factors.

Open Field Test (OFT): The motor functions of the rats and the presence of anxiety-like behavior were evaluated using the OFT. The rats were acclimated to an open-field arena measuring 80 × 80 × 40 cm for 30 min prior to testing. An infrared camera mounted on a rail at the top center of the box was used to monitor the activity of the rats, with each session lasting for 10 min. To evaluate the anxiety levels of the rats, the distance traveled by the rats in the central area of the testing arena was statistically analyzed. The total distance traveled in the entire open field was measured to assess the motor function.

Light-Dark Shuttle Test (LDT): This test involves two equal-sized compartments: One illuminated with white walls (light box) and the other completely dark with black walls (dark box). A small door connected the two boxes, allowing the rats to move freely between them. Prior to the experiment, the rats were placed in a dark box for 5 min to acclimatize to the environment. After the acclimation period, the activity was monitored for another 5 min as the mice moved between the two compartments. Anxiety levels were evaluated by recording the time spent and distance traveled in a light box within a predetermined period.

Rotation Test: All rats underwent a 3-day training period, with each session lasting 3 min, prior to the formal experiment. At the beginning of the experiment, the rats were placed on a rotating rod, and the time each rat remained on the rod was measured, with a maximum duration of 3 min. Motor function was assessed by recording the amount of time each rat spent on the rod over a 3-minute interval. The results of the training sessions served as baselines for subsequent statistical analyses.

2.5 In Vivo Bioluminescence Imaging

In vivo bioluminescence imaging was performed using an *In Vivo* Imaging System Lumina III (PerkinElmer, Waltham, MA, USA). Bioluminescence images were acquired on days 0.5, 6, 12, and 18 after BCP modeling. Prior to image acquisition, D-luciferin (Abs816138, Absin, Shanghai, China) was administered intraperitoneally, followed by 3-min inhalation of isoflurane anesthesia. Isoflurane was obtained from RWD Life Science (R510-22-10, anesthesia concentration of 2%, Shenzhen, China). Immediately after anesthesia, the rats were positioned supine in an imaging chamber for data acquisition. The intensity of the bioluminescent region was quantified as the radiance within the region of interest (ROI) and recorded after the imaging.

2.6 Three-dimensional (3D) Computed Tomography (CT) Reconstruction

CT scanning was performed on left hind limb samples from both the Sham-operated and model groups on day 18. The acquisition parameters were as follows: Spiral scanning, tube voltage of 120 kVp, slice thickness of 1 mm, and slice spacing of 1 mm. The nucleus setting was U30u, which ensured medium smoothness and a high resolution. All images were processed and analyzed using the Syngo MultiModality Workplace (MMWP) software (2007A VE22A, Erlangen, Bavaria, Germany) provided by Siemens.

2.7 Hematoxylin-eosin (H&E) Staining

Twelve days post-modeling, rats from both the Sham-operated and model groups were euthanized using pentobarbital sodium (50 mg/kg). The left tibia was fixed in 4% paraformaldehyde (BL539A, Biosharp, Hefei, Anhui, China) for 24 h and decalcified in 10% ethylenediaminetetraacetic acid (EDTA, ST066, Beyotime Biotechnology) for 24 h. Decalcified tibiae were paraffin-embedded, sectioned, and stained with H&E. Images were captured using

a microscope (Olympus BX51, Tokyo, Japan) after sealing the sections with neutral resin.

2.8 Data Collection of Harmine Downstream Proteins

Downstream proteins associated with Harmine were identified using the SwissTargetPrediction (http://swisstargetprediction.ch/) and Polypharmacology Browser (PPB) databases (https://webtools.gdb.tools/PPB/). To ensure species specificity, the filter was set to "Rattus norvegicus" for both searches. The datasets obtained from each database were thoroughly reviewed to identify Harmine-related downstream proteins while maintaining consistency in filtering criteria.

2.9 Molecular Docking

The 3D structure of Harmine was obtained from Public Chemical Database (https://pubchem.ncbi.nlm.nih.gov/), and the 3D structures and sequences of DYRK1A (Q63470) and NF-κB (Q63369) were sourced from Universal Protein Resource (https://www.uniprot.org/). AutoDock4 software (4.2.6, Scripps Research, La Jolla, CA, USA) was used for preprocessing Harmine and DYRK1A, as well as for conducting docking simulations. AlphaFold3 (alphafoldserver.com, DeepMind Technologies, London, UK) was used to predict the interaction between DYRK1A and NF-κB, and PyMOL was used to visualize docking results.

2.10 Intrathecal Cannulation

After anesthesia with sodium pentobarbital (50 mg/kg), the rats were placed in a prone position on an electric heating blanket. A 1.5 cm longitudinal incision was made over the L4-L5 spinous processes, allowing muscle separation around the L4 vertebra. The L4 spinous process was resected to expose the vertebral interspaces. A Polyethylene-10 catheter (Combio, Jiangsu, China) was carefully inserted approximately 1 cm into the subarachnoid space and securely fixed. Successful insertion was confirmed by the presence of cerebrospinal fluid (CSF) reflux. To facilitate future experiments, the distal end of the catheter was subcutaneously tunneled to the back of the rat's neck, where it was anchored and sealed to prevent CSF leakage. On the second day post-catheterization, further experiments were initiated if hindlimb weakness was observed following intrathecal injection (i.t.) of 2% lidocaine (10 µL, TCI-L0156, TCI AMERICA, Portland, OR, USA). Normal movement was expected to resume within 5 min.

2.11 Western Blot Analysis

Tissues from the lumbar enlargement of the rat SCDH were lysed in radioimmunoprecipitation assay buffer (PC101, Beyotime Biotechnology) and homogenized using a tissue homogenizer. The total protein concentration in the supernatant was measured using a Bicinchoninic Acid Protein Assay Kit (ZJ101L, Epizyme Biotech, Shanghai, China). The extracted proteins were separated using 10% sodium dodecyl sulfate-polyacrylamide gel electrophoresis and transferred onto a polyvinylidene fluoride membrane. Following blocking with a rapid blocking solution (PS108P, Epizyme Biotech), the membranes were sequentially incubated with the primary antibody, followed by the secondary antibody. Antibody detection was performed using an enhanced chemiluminescence exposure solution (SQ201, Epizyme Biotech), with specific antibody details listed in **Supplementary Material 1**.

The results were analyzed in grayscale using ImageJ software (1.4.3.67, Wayne Rasband, Bethesda, MD, USA), and the relative expression levels of the target proteins were quantified by dividing the grayscale values of the target protein bands by those of β-actin bands.

2.12 Real-time Quantitative PCR (qPCR)

Total Ribonucleic Acid (RNA) was extracted from the lumbar enlargement of the rat SCDH using TRIzol (15596018CN, Invitrogen, Waltham, MA, USA). RNA concentration was measured using a NanoDrop spectrophotometer (ND-2000, Thermo Fisher Scientific, Waltham, MA, USA). A reverse transcription kit (RR037A, Takara, Kusatsu, Shiga, Japan) was used to convert 1000 ng of RNA into complementary Deoxyribonucleic Acid (DNA). The qPCR was performed using the SYBR Green method with primers designed and synthesized by Sangon Biotech (Shanghai, China). Primer sequences are provided in **Supplementary Material 2**. Messenger RNA (mRNA) expression levels were calculated using the $2^{-\Delta\Delta CT}$ method, with data normalized to *β-actin* levels.

2.13 Enzyme-linked Immunosorbent Assay (ELISA)

The expression levels of pro-inflammatory factors in the lumbar enlargement of the rat spinal cord were measured using an ELISA kit (EK301B/4, EK306/3, EK382/3, LIANKEBIO, Hangzhou, Zhejiang, China). Optical density (OD) values were recorded at 450 and 630 nm according to the manufacturer's instructions. Calibrated OD values were obtained by subtracting the 570 nm readings from the 450 nm readings. A standard curve was generated to determine the concentrations of pro-inflammatory factors in the tissue.

2.14 Statistical Data Analysis

Statistical analyses were performed using GraphPad Prism (version 9.0, GraphPad Software, Inc., San Diego, CA, USA), and the data are presented as mean $\pm$ standard error of the mean. Comparisons between the two groups were conducted using *t*-tests, including nonparametric tests, when applicable. For comparisons among multiple groups, one- or two-way analysis of variance was used, followed by Bonferroni's post-hoc test for pairwise comparisons.

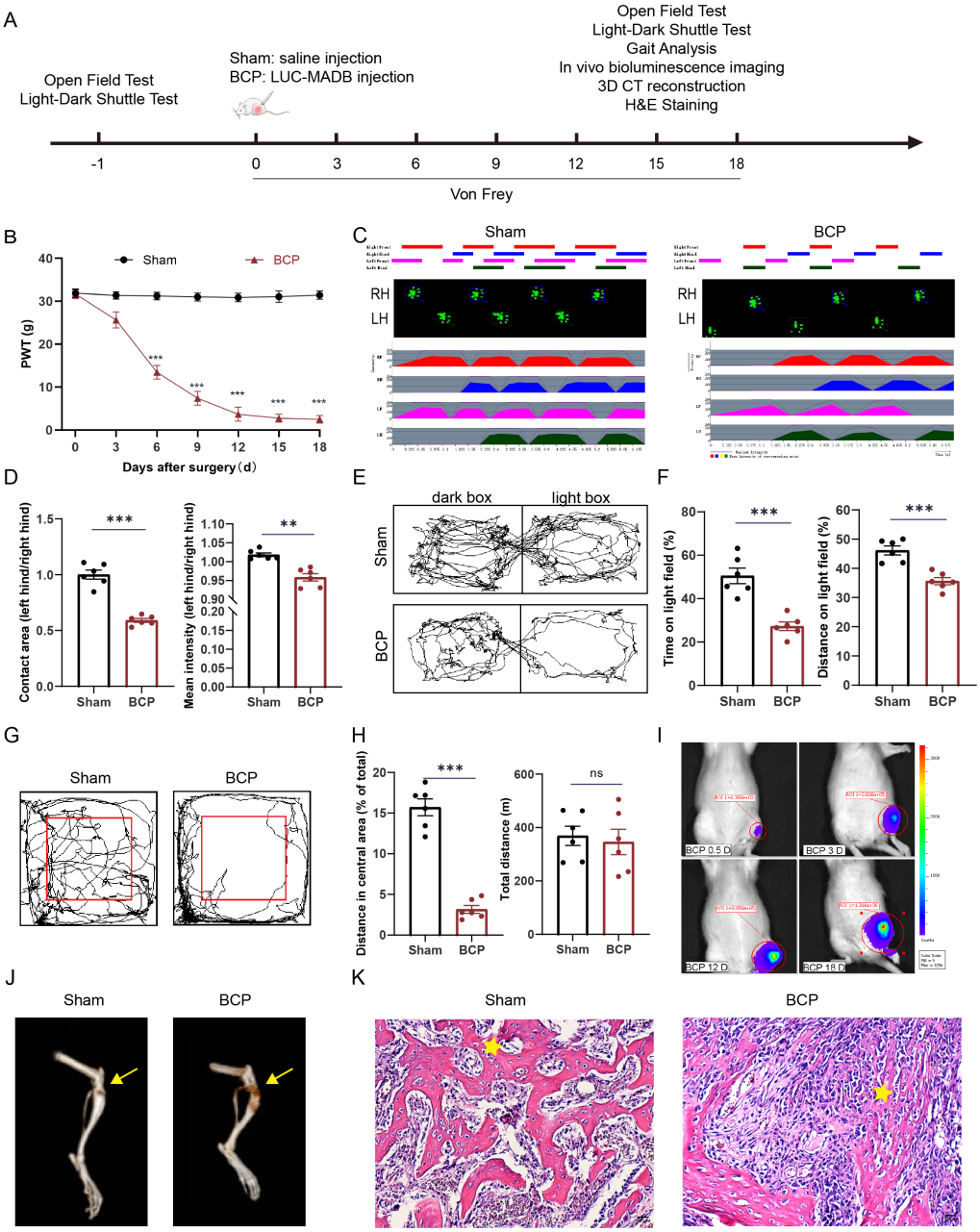

Fig. 1. BCP modeling. (A) The experimental procedures. Figure A was drawn using Adobe Illustrator 2021 software (Adobe Systems, San Jose, Ca, USA). (B) The mechanical pain threshold results demonstrated that the paw pain threshold of the rats progressively decreased from days 6 to 18 (n = 6). (C,D) Gait analysis revealed a decrease in the footprint area and mean pressure in the left hind limb in the BCP group (n = 6). LH: Left hind limb; and RH: Right hind limb. (E,F) LDT results demonstrated that the modeled group exhibited significantly reduced time and traveled a shorter distance in the bright compartment (n = 6). (G,H) The OFT revealed a significant reduction in the distance traveled by the modeled rats in the central region (n = 6). (I) Bioluminescence *in vivo* imaging revealed that following cell inoculation, the model group demonstrated cell proliferation in the tibial plateau (n = 6). (J) 3D CT images revealed extensive bone damage in the tibial plateau following model establishment, and the yellow arrows indicate the sites where cells or saline were injected during model establishment (n = 6). (K) H&E staining revealed well-preserved bone trabecular structures (indicated by pentagrams) in the Sham group, whereas in the BCP group, the bone trabecular structures exhibited significant deterioration, with extensive tumor cell infiltration observed in the bone marrow cavity (n = 6). Scale bar: 50 µm. $^{**}p < 0.01$, and $^{***}p < 0.001$ versus Sham group. BCP, bone cancer pain; H&E, hematoxylin-eosin; LDT, light-dark shuttle test; OFT, open field test; ns, mean not significant; LUC-MADB, luciferin-malignant atypical discrete breast 106 cells.

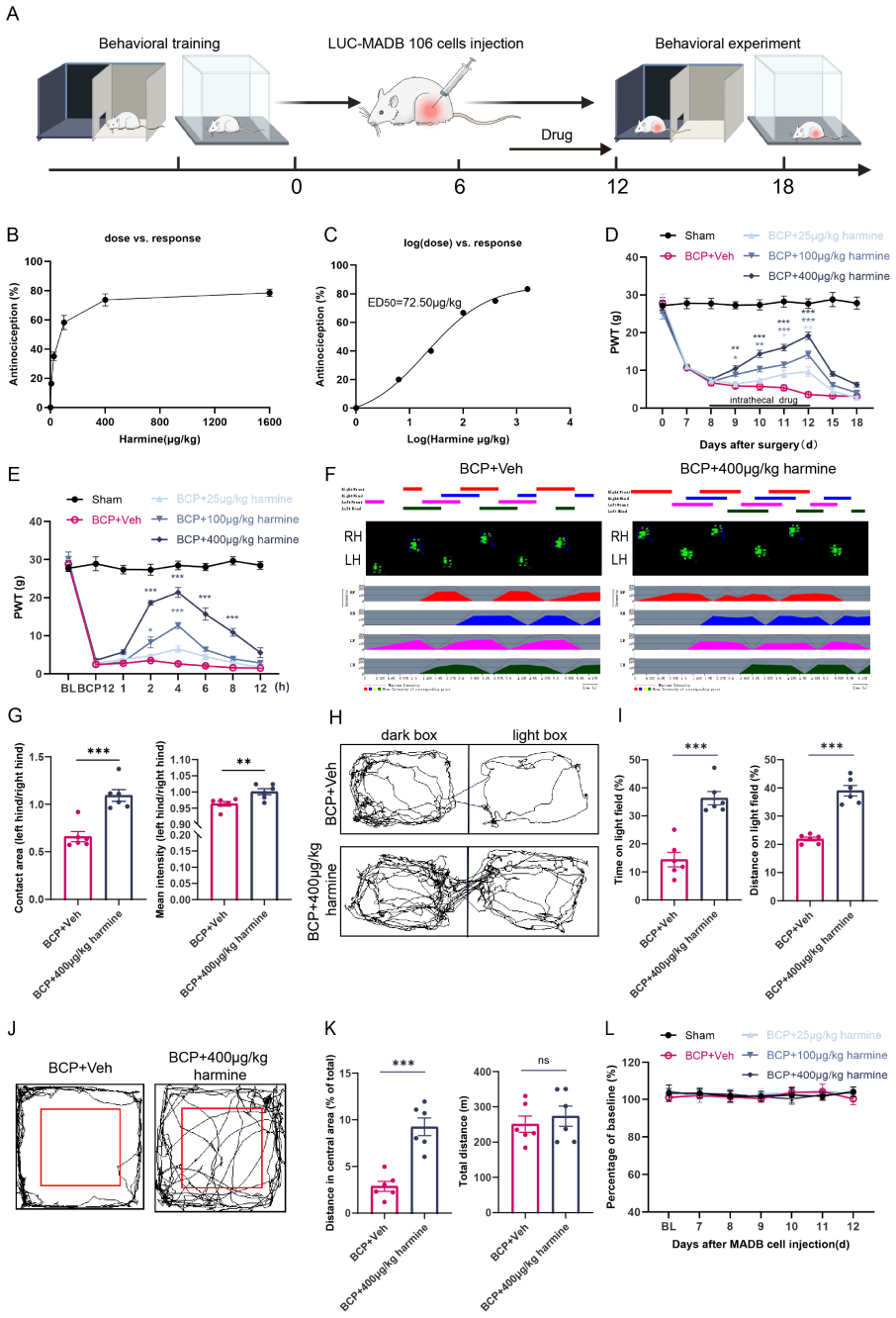

Fig. 2. Behavioral effects of intrathecal Harmine injection in rats with BCP. (A) Schematic timeline of animal experiments. Figure A was drawn using Adobe Illustrator 2021 software. (B,C) Dose-response and log (dose)-response curves of the analgesic effect following intrathecal injection of Harmine indicated that the ED_{50} for pain relief in rats with BCP was 72.50 μg/kg. (D) Intrathecal injection of Harmine relieved pain in rats with BCP in a dose- and time-dependent manner (n = 6). (E) Effect of a single injection of varying concentrations of Harmine on mechanical pain thresholds in rats with BCP was evaluated 12 days postoperatively. The analgesic effect peaked at 4 h post-injection and was sustained for up to 8 h (n = 6). (F,G) Gait analysis indicated changes in the footprint area and mean pressure on the left hind limb in the model group compared to the Harmine-treated group (n = 6). (H,I) The light-dark shuttle box experiment revealed differences in both the duration spent and distance covered in the bright box between the two groups (n = 6). (J,K) Open field experiments revealed changes in the total distance covered and the distance traveled in the central area, with the model group reporting significant differences compared to the Harmine-treated group (n = 6). (L) Rotarod test to assess the impact of different concentrations of Harmine on the motor performance of rats with BCP (n = 6). *$p < 0.05$, **$p < 0.01$, and ***$p < 0.001$ versus BCP + Veh group. ns, mean not significant; Veh, vehicle; MADB, malignant atypical discrete breast.

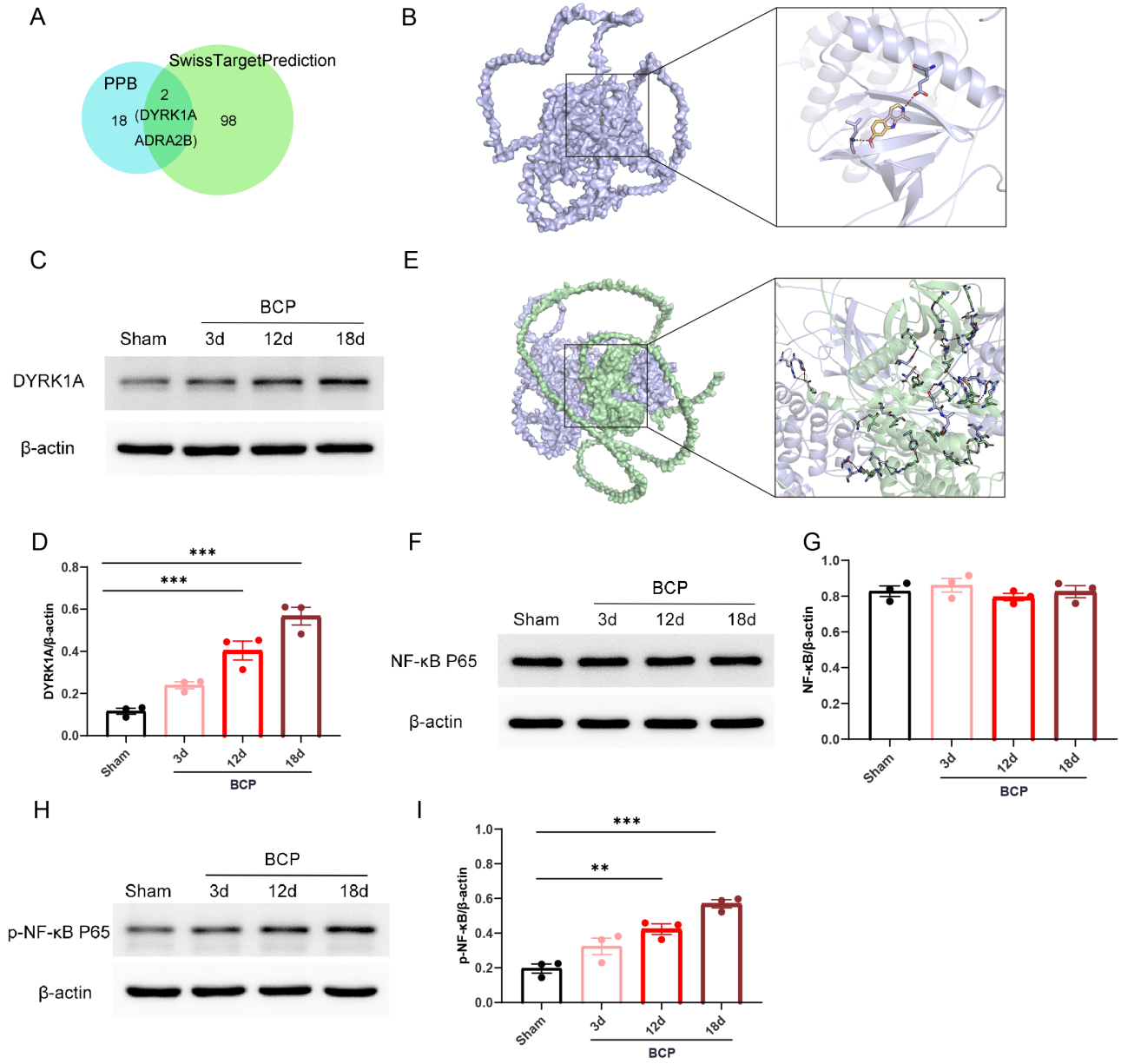

Fig. 3. Effects of bone cancer on the DYRK1A/NF-κB pathway in SCDH of rats. (A) Venn diagram demonstrating the intersection of two Harmine downstream protein datasets from both PPB and SwissTargetPrediction, identifying DYRK1A and ADRA2B. (B) Molecular docking analysis revealed hydrogen bonding between Harmine and DYRK1A, with a binding energy of –4.78 kcal/mol, indicating a moderate binding affinity. (C,D) Western blot results showed that the expression of DYRK1A in the dorsal horn of the spinal cord in the BCP model exhibited a time-dependent increase (n = 3). (E) Molecular docking analysis revealed an interaction between DYRK1A and NF-κB with increased hydrogen bonding. (F–I) Western blot results revealed that the protein expression of NF-κB did not significantly differ in SCDH in the BCP model, whereas the protein expression of p-NF-κB was proportional to time (n = 3). $^{**}p < 0.01$, and $^{***}p < 0.001$ versus Sham group. PPB, Polypharmacology Browser; DYRK1A, dual-specificity tyrosine phosphorylation-regulated kinase 1A; ADRA2B, Adrenoceptor Alpha 2B; NF-κB, nuclear factor kappa-light-chain-enhancer of activated B cells; SCDH, spinal cord dorsal horn; p-NF-κB, polyclonal-NF-κB.

3. Results

3.1 Tibial Inoculation of LUC-MADB Breast Cancer Cells Induces Abnormal Mechanical Pain in Rats

To confirm the successful establishment of the BCP model, we performed a thorough evaluation of rats in both the Sham and BCP groups, assessing their paw pain thresholds, motor function, and pain-related emotional behaviors. The specific experimental procedures are shown in Fig. 1A. Pain thresholds were measured using the Von Frey test. The results revealed a significant reduction in pain thresholds in

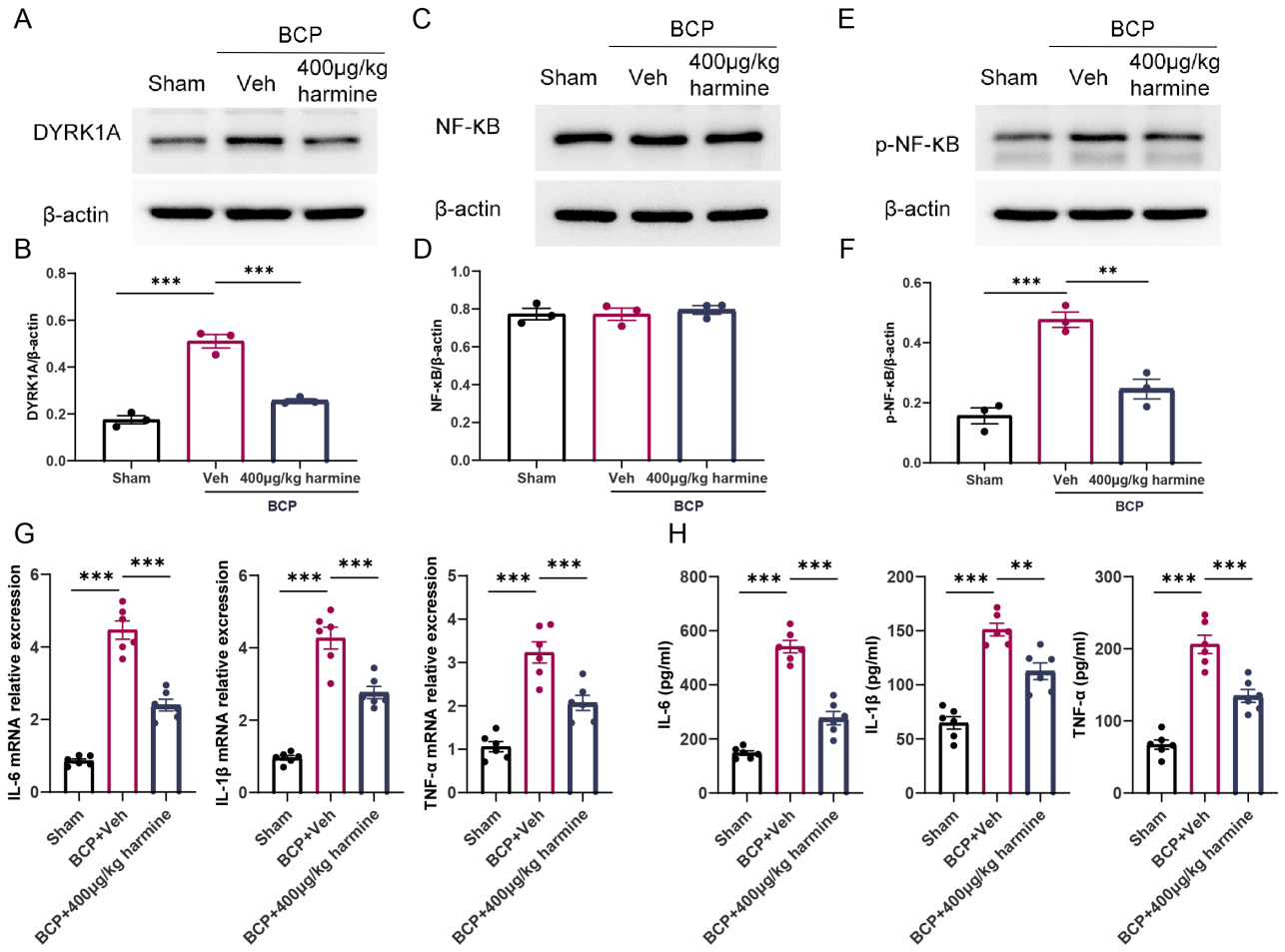

Fig. 4. Harmine modulates the DYRK1A/NF-κB signaling pathway in rats with BCP. (A–F) Western blot analysis indicated that DYRK1A expression was reduced, the protein expression of NF-κB reported no significant difference, and the protein expression of p-NF-κB was lower in the Harmine-treated group compared to the BCP + Veh group (n = 3). (G) qPCR and (H) ELISA were conducted to assess the impact of Harmine on the expression of pro-inflammatory factors induced by BCP (n = 6). $^{**}p < 0.01$, and $^{***}p < 0.001$ versus BCP + Veh group. ns, mean not significant; qPCR, real-time quantitative PCR; ELISA, Enzyme-linked Immunosorbent Assay.

the BCP group by day 6 compared to the Sham group, with this reduction stabilizing by day 12 (Fig. 1B). Gait analysis indicated that limb motor function remained intact in both groups; however, the footprint area and average pressure of the left hind paw were significantly reduced in the BCP group (Fig. 1C,D). Light-dark shuttle box experiments demonstrated that the BCP group spent less time in the light box and covered a shorter distance than the Sham group (Fig. 1E,F). OFT results indicated no significant difference in the total distance traveled between the two groups during the first 5 min of movement. However, the BCP group exhibited a greater tendency to walk along the walls of the box, with significantly reduced distance traveled in the central area and diminished exploratory behavior compared to the Sham group (Fig. 1G,H). These behavioral experiments demonstrated that the modeled rats developed heightened pain sensitivity and negative emotional behaviors related to their pain perception. Fluorescence *in vivo* imaging revealed a progressive enhancement of fluorescence signals in rats following BCP modeling (Fig. 1I). 3D CT scans indicated that the BCP group rats exhibited damage to the tibial plateau compared to the Sham group, revealing severe bone destruction (Fig. 1J). H&E staining results from tibial plateau slices indicated that compared to the Sham group, the morphology of bone trabeculae in the BCP group was altered, with significant tumor cell invasion (Fig. 1K). In summary, these experiments confirmed that tumor cells infiltrated the bone marrow cavity and proliferated extensively, leading to bone destruction and pain. Additionally, the morphological analyses also validated the successful establishment of the BCP animal model.

3.2 Harmine Ameliorates Nociceptive Hypersensitivity and Pain-related Negative Emotional Behavior in Rats With BCP in a Dose-dependent Manner

To evaluate the efficacy of Harmine in alleviating pain in rats with BCP, varying concentrations of Harmine solution (6.25, 25, 100, 400, and 1600 μg/kg) were adminis-

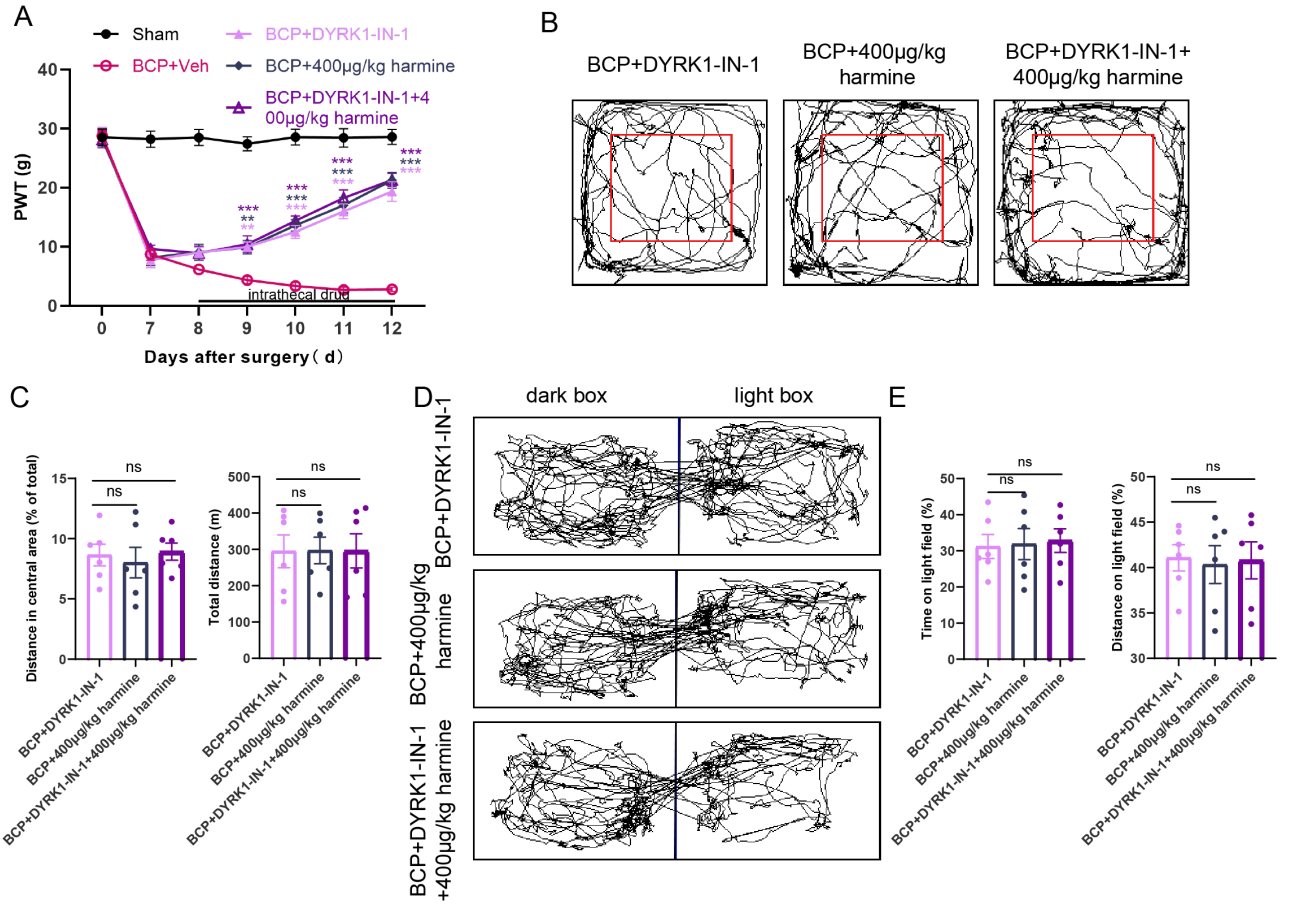

Fig. 5. Effects of intrathecal injection of DYRK1-IN-1 and Harmine on pain behavior in rats with BCP. (A) Von Frey test was used to evaluate the effects of BCP + DYRK1-IN-1, BCP + Harmine, and BCP + DYRK1-IN-1 + Harmine on pain thresholds in rats with BCP (n = 6). (B,C) OFT detected changes in the total distance covered and the distance traversed in the central area by the three groups of rats (n = 6). (D,E) LDT detected changes in the duration and distance traveled in the bright box among the three groups of rats (n = 6). $^{**}p < 0.01$, and $^{***}p < 0.001$ versus BCP + Veh group. ns, mean not significant.

tered via intrathecal injection daily from days 8 to 12 post-modeling. Behavioral assessments were then performed (Fig. 2A). Log (dose)-response curves were generated based on different concentrations of Harmine (Fig. 2B), and log (dose)-response curves were plotted, leading to the calculation of the half-effective dose (ED_{50}) of 72.50 μg/kg (Fig. 2C). Behavioral assays were conducted to explore the pain-relieving effects of Harmine on BCP. The results revealed that administering Harmine at doses of 25, 100, and 400 μg/kg led to a progressive increase in the pain thresholds of the rats, demonstrating both time- and dose-dependent effects. Notably, the pain thresholds in the group receiving the 400 μg/kg intrathecal injection of Harmine demonstrated significant restoration, with the analgesic effect persisting even after the cessation of Harmine administration (Fig. 2D).

The onset and duration of the action of Harmine were further investigated through a single administration on the 12th day post-modeling. The 25 μg/kg Harmine group did not exhibit a significant therapeutic effect on the pain thresholds of rats after this single administration. In contrast, the 100 and 400 μg/kg Harmine groups demonstrated an onset of effect 2 h after injection, with the drug's effect peaking at 4 h and maintaining efficacy until 8 h post-administration. The pain thresholds of the rats exhibited a dose-dependent increase that was sustained for 8 h (Fig. 2E). Additionally, the pain-relieving effects of Harmine on spontaneous pain in rats with BCP were assessed using gait analysis. The findings revealed that 12 days post-surgery, the Harmine-treated group (400 μg/kg, i.t.) demonstrated significant improvement in key indicators of the left hind paw (Fig. 2F,G). To evaluate whether Harmine alleviates BCP-induced negative emotional behaviors associated with pain, we performed the LDT. The results indicated that compared with the BCP + Vehicle (Veh) group, the Harmine-treated group (400 μg/kg, i.t.) showed a marked rise in both the time in the light box and traveled a greater distance (Fig. 2H,I). Furthermore, exploratory activity of BCP rats was assessed using the OFT, which revealed that rats in the Harmine-treated group exhibited increased time in the central area compared to the BCP + Veh group (Fig. 2J,K). Collectively, these experi-

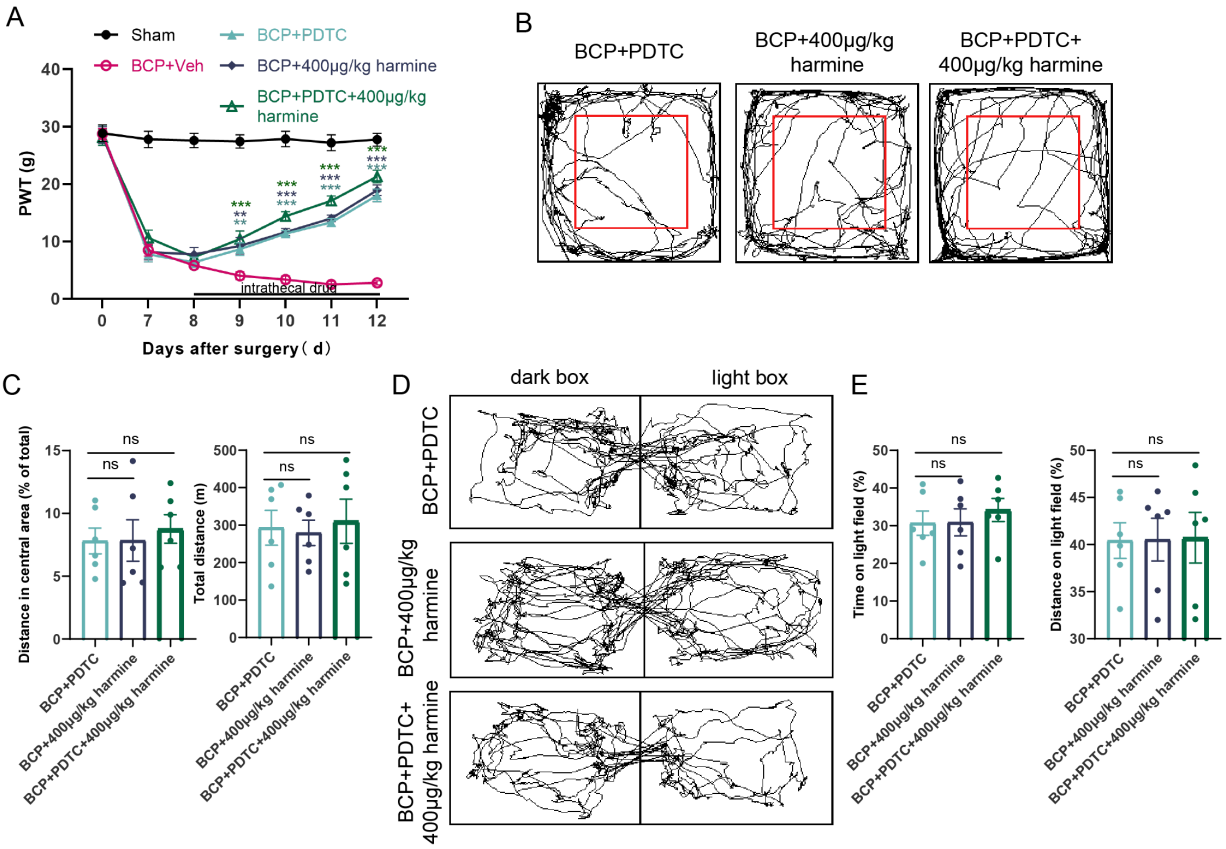

Fig. 6. Effects of intrathecal injection of PDTC and Harmine on pain behavior in rats with BCP. (A) Von Frey test was used to evaluate the effects of BCP + PDTC, BCP + Harmine, and BCP + PDTC + Harmine on pain thresholds in rats with BCP (n = 6). (B,C) OFT detected changes in the total distance covered and the distance traversed in the central area by the three groups of rats (n = 6). (D,E) LDT detected changes in the duration and distance traveled in the bright box among the three groups of rats (n = 6). $^{**}p < 0.01$, and $^{***}p < 0.001$ versus BCP + Veh group. ns, mean not significant; PDTC, pyrrolidinedithiocarbamate.

ments demonstrated that Harmine alleviated BCP-induced nociceptive hypersensitivity and reduced pain-related negative emotional behaviors. Notably, the results of the rotarod test confirmed that intrathecal injection of Harmine did not impair motor function in rats, thereby demonstrating its safety (Fig. 2L).

3.3 DYRK1A/NF-κB Signaling Axis May Be Involved in Harmine-mediated Alleviation of BCP

The downstream proteins of Harmine were identified using the SwissTargetPrediction and PPB databases, which led to the identification of common proteins, specifically DYRK1A and Adrenoceptor Alpha 2B (ADRA2B) (Fig. 3A). Previous studies have indicated that central neuroinflammatory mechanisms play a critical role in BCP pathogenesis [29,30]. Consequently, we selected DYRK1A, known for its anti-inflammatory properties and anxiolytic effects, as the downstream protein of Harmine for further investigation. To validate these predictions, molecular docking studies were performed, which revealed hydrogen bonding between Harmine and DYRK1A, indicating a moderate binding affinity (Fig. 3B). Further analysis of DYRK1A protein levels in the SCDH of rats with BCP further demonstrated a time-dependent upregulation of expression (Fig. 3C,D). Additionally, considering that DYRK1A has been shown to facilitate the activation of NF-κB [31], predictions made using AlphaFold3 indicated an increased number of hydrogen bonds between DYRK1A and NF-κB, suggesting a stronger interaction between the two (Fig. 3E). This led to the hypothesis that NF-κB may serve as a downstream effector of DYRK1A. A time-dependent increase in NF-κB activity was observed in the BCP model using Western blot (Fig. 3C–I), supporting the involvement of the DYRK1A/NF-κB signaling axis in BCP. All original WB images in Fig. 3C,F,H are provided in **Supplementary Material 3**.

3.4 Harmine Modulates the DYRK1A/NF-κB Signaling Axis in the SCDH of Rats With BCP

To verify that Harmine regulates the DYRK1A/NF-κB signaling axis, we assessed the expression levels of DYRK1A, NF-κB, and polyclonal-NF-κB (p-NF-κB) in the SCDH of rats with BCP following Harmine treatment (400 μg/kg, i.t.). Comparison of the results re-

vealed a marked decrease in DYRK1A expression in the SCDH of BCP-treated rats compared with Harmine (Fig. 4A,B). The expression of total NF-κB remained unchanged (Fig. 4C,D), whereas that of p-NF-κB was notably decreased (Fig. 4E,F). All original WB images in Fig. 4A,C, and E are provided in **Supplementary Material 3**. These findings demonstrate that Harmine reversed the upregulation of DYRK1A/NF-κB signaling axis-related molecules induced by bone cancer. Pain is often accompanied by the secretion of inflammatory factors, which not only enhance the sensitivity of nociceptors, exacerbating pain perception but also participate in amplifying and sustaining local inflammatory responses, thereby promoting the development and persistence of pain [32]. The qPCR and ELISA assays revealed that modeling significantly increased the protein levels of the inflammatory factors Interleukin-6 (IL-6), Interleukin-1beta (IL-1β), and Tumor Necrosis Factor-alpha (TNF-α). However, Harmine treatment significantly reduced the protein expression of these inflammatory factors in SCDH cells (Fig. 4G,H). Collectively, these experiments revealed that Harmine can suppress NF-κB inflammatory signaling pathway activation and reduce the release of inflammatory factors in SCDH. All original data for PCR and ELISA are provided in **Supplementary Materials 4,5**.

3.5 The DYRK1A/NF-κB Signaling Pathway Is Associated With the Therapeutic Effects of Harmine on Hyperalgesia and Pain-induced Negative Emotional Behaviors in BCP Rats

To further elucidate the role of the DYRK1A/NF-κB signaling axis in Harmine's regulation of hyperalgesia in rats with BCP, intrathecal injection of the DYRK1A inhibitor, DYRK1-IN-1, was administered to rats with BCP to achieve knockdown of DYRK1A. It was found that the pain thresholds of rats with BCP increased following DYRK1A inhibition, consistent with the effect observed in the BCP + Harmine group. To investigate whether DYRK1A and other molecules are therapeutic targets of Harmine for BCP, a BCP + DYRK1-IN-1 + Harmine group was included. The results reported no significant difference in analgesic effects among DYRK1-IN-1 + Harmine-, Harmine-, and DYRK1-IN-1-treated groups (Fig. 5A).

In addition to assessing mechanical pain thresholds, we evaluated the anxiety levels of the rats in each group using behavioral tests. The OFT results demonstrated that all groups maintained intact motor function without significant differences in the total distance traveled within the same time period. Moreover, the rats' desire to explore the central region was restored in all three groups, with no significant differences among them (Fig. 5B,C). Similarly, the LDT results indicated no significant differences among the three groups in terms of time spent and distance traveled in the light box, suggesting that all three treatments exerted anxiolytic effects (Fig. 5D,E).

These findings demonstrate that the inhibition of DYRK1A by DYRK1-IN-1 and administering Harmine produced consistent effects, alleviating pain and anxiety-like behaviors in rats with BCP. Co-administration of DYRK1-IN-1 and Harmine did not enhance the analgesic effects on BCP or pain-related negative emotional behaviors. Similar experiments targeting NF-κB within the DYRK1A/NF-κB signaling axis produced consistent results such that both suppression of NF-κB by PDTC and administration of Harmine alleviated pain and anxiety-like behaviors in rats with BCP. Furthermore, co-administration of PDTC and Harmine failed to enhance the analgesic effects of BCP (Fig. 6). The above results indicate that the DYRK1A/NF-κB signaling pathway is involved in the analgesic effects of Harmine in the BCP model.

4. Discussion

BCP is a significant clinical challenge that profoundly affects the quality of life of patients with advanced malignancies. The findings of this study provide compelling evidence that Harmine, a β-carboline alkaloid derived from *Peganum harmala*, exhibits notable analgesic effects in a rat model of BCP. This study investigated the analgesic effects of Harmine in a rat model of BCP and explored the underlying mechanisms. Our results demonstrated that Harmine alleviates mechanical allodynia and pain-related negative emotional behavior in rats with BCP in a dose-dependent manner. In addition, we also found that the DYRK1A/NF-κB signaling pathway is closely related to the analgesic effects of Harmine.

The underlying mechanisms of the analgesic effects of Harmine appear to be closely linked to the modulation of the DYRK1A/NF-κB signaling pathway. DYRK1A, a dual-specificity kinase, is implicated in various cellular processes, including inflammation and neuronal signaling [22,33]. Our study demonstrated that Harmine significantly reduced DYRK1A expression in the SCDH of rats with BCP, which correlated with a decrease in the activation of the NF-κB pathway. This is particularly relevant because NF-κB is a pivotal transcription factor involved in the regulation of pro-inflammatory cytokines and mediators that contribute to pain sensitization.

Inflammatory factors and chronic pain mechanisms interact in complex ways. Inflammatory mediators are released in response to injury or disease, and these factors not only directly enhance the sensitivity of nociceptors but also promote and sustain chronic pain through various mechanisms. Our findings indicate that Harmine not only inhibits the activation of DYRK1A but also reduces the expression of inflammatory cytokines, such as IL-6, IL-1β, and TNF-α, in SCDH. This suggests that Harmine may exert its analgesic effects by modulating glial cell activity and reducing neuroinflammation, thereby interrupting the cycle of pain amplification.

Furthermore, the behavioral assessments conducted in this study revealed that Harmine treatment not only alleviated mechanical hypersensitivity but also mitigated anxiety-like behaviors associated with chronic pain. OFT and LDT results indicated that Harmine-treated rats exhibited increased exploratory behavior, suggesting an improvement in their overall emotional state. This is particularly important because chronic pain is often accompanied by psychological distress that can complicate treatment outcomes.

While this study provides valuable insights into the analgesic properties of Harmine, it is essential to address certain limitations. This study primarily focused on a rat model of BCP, and further studies are needed to evaluate the translational potential of these findings in human subjects. Additionally, the long-term effects of Harmine and its safety profile require thorough investigation to establish its viability as a clinical treatment option.

5. Conclusion

Our study provides compelling evidence that Harmine exerts significant analgesic effects in a rat model of BCP, which correlates with the suppression of the DYRK1A/NF-κB signaling axis. These findings provide a solid foundation for developing novel therapeutic strategies targeting BCP.

Availability of Data and Materials

Data will be made available upon request.

Author Contributions

SYZ: the acquisition, analysis, and interpretation of data. SZ: the acquisition and analysis of data, YL, LC, JL and JJ: the acquisition of data. MY: design of the work, funding acquisition, project administration, supervision. LX: design of the work, funding acquisition, project administration, supervision, writing – review & editing. All authors contributed to editorial changes in the manuscript. All authors read and approved the final manuscript. All authors have participated sufficiently in the work and agreed to be accountable for all aspects of the work.

Ethics Approval and Consent to Participate

These experiments were approved by the Institutional Animal Care and Use Committee of Jiaxing University (Ethical Approval No. JUMC2021-093) and were conducted in strict adherence to the guidelines set forth by the International Association for the Study of Pain for the care and use of laboratory animals. All experimental protocols were approved by the Animal Care and Use Committee of Jiaxing University and were performed following the guidelines of the National Institutes of Health.

Acknowledgment

Not applicable.

Funding

The study was supported, in part, by grants from the Natural Science Foundation of Zhejiang Province (LTGC23H090002), National Natural Science Foundation of China (82171216), People's Livelihood Science and Technology Innovation Research Project of Jiaxing City (2023AY31025), Clinical Key Specialties of Zhejiang Province -Anesthesiology (2023-ZJZK-001) and National Clinical Key Specialties-Oncology (2023-GJZK-001).

Conflict of Interest

The authors declare no conflict of interest.

Supplementary Material

Supplementary material associated with this article can be found, in the online version, at https://doi.org/10.31083/JIN38100.

References

[1] Ismy J, Emril DR, Rizkidawati. Management of cancer pain with analgetic adjuvant and weak opioid in prostate cancer bone metastases: A case series. Annals of Medicine and Surgery (2012). 2020; 60: 575–578. https://doi.org/10.1016/j.amsu.2020.10.070.

[2] Bindels BJJ, Mercier C, Gal R, Verlaan JJ, Verhoeff JJC, Dirix P, *et al*. Stereotactic Body and Conventional Radiotherapy for Painful Bone Metastases: A Systematic Review and Meta-Analysis. JAMA Network Open. 2024; 7: e2355409. https://doi.org/10.1001/jamanetworkopen.2023.55409.

[3] Smith HS. Painful osseous metastases. Pain Physician. 2011; 14: E373–403.

[4] Siegel GW, Biermann JS, Calinescu AA, Spratt DE, Szerlip NJ. Surgical Approach to Bone Metastases. Current Osteoporosis Reports. 2018; 16: 512–518. https://doi.org/10.1007/s11914-018-0463-7.

[5] Wang K, Donnelly CR, Jiang C, Liao Y, Luo X, Tao X, *et al*. STING suppresses bone cancer pain via immune and neuronal modulation. Nature Communications. 2021; 12: 4558. https://doi.org/10.1038/s41467-021-24867-2.

[6] Prommer EE. Pharmacological Management of Cancer-Related Pain. Cancer Control: Journal of the Moffitt Cancer Center. 2015; 22: 412–425. https://doi.org/10.1177/107327481502200407.

[7] Afsharimani B, Kindl K, Good P, Hardy J. Pharmacological options for the management of refractory cancer pain-what is the evidence? Supportive Care in Cancer: Official Journal of the Multinational Association of Supportive Care in Cancer. 2015; 23: 1473–1481. https://doi.org/10.1007/s00520-015-2678-9.

[8] Koob GF. Neurobiology of Opioid Addiction: Opponent Process, Hyperkatifeia, and Negative Reinforcement. Biological Psychiatry. 2020; 87: 44–53. https://doi.org/10.1016/j.biopsych.2019.05.023.

[9] Beth-Tasdogan NH, Mayer B, Hussein H, Zolk O, Peter JU. Interventions for managing medication-related osteonecrosis of the jaw. The Cochrane Database of Systematic Reviews. 2022; 7: CD012432. https://doi.org/10.1002/14651858.CD012432.pub3.

[10] Panchal NK, Prince Sabina E. Non-steroidal anti-inflammatory drugs (NSAIDs): A current insight into its molecular mechanism eliciting organ toxicities. Food and Chemical Toxicology: an International Journal Published for the British Indus-

trial Biological Research Association. 2023; 172: 113598. https://doi.org/10.1016/j.fct.2022.113598.

[11] Yang B, Zhang Z, Yang Z, Ruan J, Luo L, Long F, *et al*. Chanling Gao Attenuates Bone Cancer Pain in Rats by the IKKβ/NF-κB Signaling Pathway. Frontiers in Pharmacology. 2020; 11: 525. https://doi.org/10.3389/fphar.2020.00525.

[12] Song ZP, Xiong BR, Guan XH, Cao F, Manyande A, Zhou YQ, *et al*. Minocycline attenuates bone cancer pain in rats by inhibiting NF-κB in spinal astrocytes. Acta Pharmacologica Sinica. 2016; 37: 753–762. https://doi.org/10.1038/aps.2016.1.

[13] Yang H, Wu L, Deng H, Chen Y, Zhou H, Liu M, *et al*. Anti-inflammatory protein TSG-6 secreted by bone marrow mesenchymal stem cells attenuates neuropathic pain by inhibiting the TLR2/MyD88/NF-κB signaling pathway in spinal microglia. Journal of Neuroinflammation. 2020; 17: 154. https://doi.org/10.1186/s12974-020-1731-x.

[14] Qi JY, Jin YC, Wang XS, Yang LK, Lu L, Yue J, *et al*. Ruscogenin Exerts Anxiolytic-Like Effect via Microglial NF-κB/MAPKs/NLRP3 Signaling Pathways in Mouse Model of Chronic Inflammatory Pain. Phytotherapy Research: PTR. 2024; 38: 5417–5440. https://doi.org/10.1002/ptr.8325.

[15] Wang J, Yin C, Pan Y, Yang Y, Li W, Ni H, *et al*. CXCL13 contributes to chronic pain of a mouse model of CRPS-I via CXCR5-mediated NF-κB activation and pro-inflammatory cytokine production in spinal cord dorsal horn. Journal of Neuroinflammation. 2023; 20: 109. https://doi.org/10.1186/s12974-023-02778-x.

[16] Giraud F, Pereira E, Anizon F, Moreau P. Recent Advances in Pain Management: Relevant Protein Kinases and Their Inhibitors. Molecules (Basel, Switzerland). 2021; 26: 2696. https://doi.org/10.3390/molecules26092696.

[17] Moloudizargari M, Mikaili P, Aghajanshakeri S, Asghari MH, Shayegh J. Pharmacological and therapeutic effects of Peganum harmala and its main alkaloids. Pharmacognosy Reviews. 2013; 7: 199–212. https://doi.org/10.4103/0973-7847.120524.

[18] Kadyan P, Singh L. Unraveling the mechanistic interplay of mediators orchestrating the neuroprotective potential of harmine. Pharmacological Reports: PR. 2024; 76: 665–678. https://doi.org/10.1007/s43440-024-00602-8.

[19] Zhang L, Li D, Yu S. Pharmacological effects of harmine and its derivatives: a review. Archives of Pharmacal Research. 2020; 43: 1259–1275. https://doi.org/10.1007/s12272-020-01283-6.

[20] Zheng ZH, Lin XC, Lu Y, Cao SR, Liu XK, Lin D, *et al*. Harmine exerts anxiolytic effects by regulating neuroinflammation and neuronal plasticity in the basolateral amygdala. International Immunopharmacology. 2023; 119: 110208. https://doi.org/10.1016/j.intimp.2023.110208.

[21] Habib MZ, Tadros MG, Abd-Alkhalek HA, Mohamad MI, Eid DM, Hassan FE, *et al*. Harmine prevents 3-nitropropionic acid-induced neurotoxicity in rats via enhancing NRF2-mediated signaling: Involvement of p21 and AMPK. European Journal of Pharmacology. 2022; 927: 175046. https://doi.org/10.1016/j.ejphar.2022.175046.

[22] Ju C, Wang Y, Zang C, Liu H, Yuan F, Ning J, *et al*. Inhibition of Dyrk1A Attenuates LPS-Induced Neuroinflammation via the TLR4/NF-κB P65 Signaling Pathway. Inflammation. 2022; 45: 2375–2387. https://doi.org/10.1007/s10753-022-01699-w.

[23] Göckler N, Jofre G, Papadopoulos C, Soppa U, Tejedor FJ, Becker W. Harmine specifically inhibits protein kinase DYRK1A and interferes with neurite formation. The FEBS Journal. 2009; 276: 6324–6337. https://doi.org/10.1111/j.1742-4658.2009.07346.x.

[24] Khor B, Gagnon JD, Goel G, Roche MI, Conway KL, Tran K, *et al*. The kinase DYRK1A reciprocally regulates the differentiation of Th17 and regulatory T cells. eLife. 2015; 4: e05920. https://doi.org/10.7554/eLife.05920.

[25] Lauria PSS, Gomes JDM, Abreu LS, Santana RC, Nunes VLC, Couto RD, *et al*. Ayahuasca and its major component harmine promote antinociceptive effects in mouse models of acute and chronic pain. Journal of Ethnopharmacology. 2024; 323: 117710. https://doi.org/10.1016/j.jep.2024.117710.

[26] Fu J, Zhao B, Ni C, Ni H, Xu L, He Q, *et al*. Rosiglitazone Alleviates Mechanical Allodynia of Rats with Bone Cancer Pain through the Activation of PPAR-γ to Inhibit the NF-κB/NLRP3 Inflammatory Axis in Spinal Cord Neurons. PPAR Research. 2021; 2021: 6086265. https://doi.org/10.1155/2021/6086265.

[27] Kuang J, Xu M, Xu C, Wang Y, Ni C, Wei S, *et al*. miR-199a-3p mediates bone cancer pain through upregulation of dnmt3a expression in spinal dorsal horn neurons. Biochemical and Biophysical Research Communications. 2023; 682: 97–103. https://doi.org/10.1016/j.bbrc.2023.09.069.

[28] Xu M, Fei Y, He Q, Fu J, Zhu J, Tao J, *et al*. Electroacupuncture Attenuates Cancer-Induced Bone Pain via NF-κB/CXCL12 Signaling in Midbrain Periaqueductal Gray. ACS Chemical Neuroscience. 2021; 12: 3323–3334. https://doi.org/10.1021/acschemneuro.1c00224.

[29] Ding Y, He J, Huang J, Yu T, Shi X, Zhang T, *et al*. Harmine induces anticancer activity in breast cancer cells via targeting TAZ. International Journal of Oncology. 2019; 54: 1995–2004. https://doi.org/10.3892/ijo.2019.4777.

[30] Zhang H, Sun K, Ding J, Xu H, Zhu L, Zhang K, *et al*. Harmine induces apoptosis and inhibits tumor cell proliferation, migration and invasion through down-regulation of cyclooxygenase-2 expression in gastric cancer. Phytomedicine: International Journal of Phytotherapy and Phytopharmacology. 2014; 21: 348–355. https://doi.org/10.1016/j.phymed.2013.09.007.

[31] Li Y, Xie X, Jie Z, Zhu L, Yang JY, Ko CJ, *et al*. DYRK1a mediates BAFF-induced noncanonical NF-κB activation to promote autoimmunity and B-cell leukemogenesis. Blood. 2021; 138: 2360–2371. https://doi.org/10.1182/blood.2021011247.

[32] Baral P, Udit S, Chiu IM. Pain and immunity: implications for host defence. Nature Reviews. Immunology. 2019; 19: 433–447. https://doi.org/10.1038/s41577-019-0147-2.

[33] Shen J, Zhang P, Li Y, Fan C, Lan T, Wang W, *et al*. Neuroprotective effects of microRNA-211-5p on chronic stress-induced neuronal apoptosis and depression-like behaviours. Journal of Cellular and Molecular Medicine. 2021; 25: 7028–7038. https://doi.org/10.1111/jcmm.16716.